J Mater Sci (2010) 45:2843–2851
DOI 10.1007/s10853-010-4224-y

The anisotropy of ac conductivity and dielectric constant of anisotropic conductor–insulator composites

Yuichi Hazama · Jun Nakamura · Akiko Natori

Received: 30 November 2008 / Accepted: 10 December 2009 / Published online: 2 February 2010

Abstract We study the complex ac admittance tensor (ac conductivity and dielectric constant) of anisotropic conductor–insulator composite materials, based on anisotropic two-dimensional *RC*-networks consisting of randomly placed conductors and capacitors with different conductor existence (bond occupation) probabilities in two directions. We calculate numerically each component of the complex ac admittance tensor by applying a transfer matrix method and reveal the effect of the anisotropy of the bond occupation probability on the frequency characteristics of the ac admittance tensor. It is found that the dual relation holds for each diagonal component of the complex admittance tensor of the anisotropic two-dimensional *RC*-network. For the effective conductance in the metallic region, the anisotropy depends not only on the anisotropy of the bond occupation probability, but also on the frequency ω. We derive the analytical relation between the anisotropy of the conductance and the anisotropy of the bond occupation probability, at both the dc limit and $\omega\, RC = 1$. The calculated results on the ac admittance are compared with the effective medium theory and how the accuracy of the theory is related with the microscopic current path is clarified.

Introduction

Recently, conductor–insulator composite materials such as metal-filled epoxy adhesives have been increasingly expected as a promising candidate instead of solder in microelectronics field [1]. Here, the high frequency ac conductive and dielectric properties are essentially important.

With respect to ac conductivity and dielectric constant of a conductor–insulator composite, experimental studies have been mainly performed near the percolation threshold from scientific interests [2–4]. Ac-conductivity measurement in a wide frequency range of 5 Hz–13 MHz has been performed in a metallic region for $La_2NiO_{4+\delta}$ with quasi-two-dimensional structure [5]. The observed ac conductivity is constant at low frequencies, and increases by the power law and saturates at high frequencies. Recently, ac and dc percolative conductivity has been measured on magnetite–cellulose acetate composites in a wide range of volume fraction from a metallic region to an insulating region [6]. The observed ac conductivity in a metallic region is constant at low frequencies and increases by the power law in a frequency range of 10^{-2} to 3×10^6 Hz, while it is decreased by the power law with decreasing frequency in an insulating region.

The properties of isotropic conductor–insulator composites have been extensively studied by both experimental and theoretical physics for many years [7]. Effective medium theory [8, 9] was used to analyze the data, but since the 1970s, one of the main theoretical models has involved percolation theory and the concept of scaling [10–12]. Some powerful numerical methods to obtain the critical exponent near the percolation threshold have been developed, such as a transfer matrix approach [13], a position-space renormalization group [14], and efficient Monte Carlo algorithm [15]. Percolation theory predicts a universal behavior of the electrical conductivity and the dielectric properties, which does not depend on details of the system but the spatial dimension. Actually,

Y. Hazama · J. Nakamura · A. Natori (✉)
Department of Electronic-Engineering, The University of Electro-Communications, 1-5-1 Chofugaoka, Chofu, Tokyo 182-8585, Japan
e-mail: natori@ee.uec.ac.jp

behavior of percolation clusters was directly observed in sintered mixture of niobium and alumina with an image processing system [16]. Kinetic roughening of charge spreading has also been detected in a two-dimensional silicon nano-crystal network by electrostatic force microscopy [17].

Recently, on the other hand, fine particles with a high aspect ratio have been expected as the filler to reduce the percolation threshold. A polysterene–graphene composite exhibits a percolation threshold of only $\sim$0.1 volume percent for the room temperature electrical conductivity [18]. A graphene has two-dimensional structure and the observed conductivity exhibits slight anisotropy. Carbon nanotubes filled polymetric materials have also been expected as conducting composite material with the low percolation threshold [19, 20]. The electrical conductivity depends not only on the concentration, but also on the alignment and either dependence exhibits the critical power-law behavior [20]. In the aligned case, strong anisotropy on the dc conductance has been observed [20]. However, the interrelation between the geometrical anisotropy of the composite material and the anisotropy of the conductance has not been sufficiently clarified.

With respect to the anisotropy of dc conductance, a two-dimensional square random resistor network has been studied with two models; an anisotropic resistor model with anisotropic conductance in two directions and an anisotropic percolation model with anisotropic bond occupation probabilities in two directions. In the former anisotropic resistor model, it is pointed out that the anisotropy in the macroscopic conductance vanishes in the vicinity of the percolation threshold [21, 22]. Actually, metal islands with controllable anisotropy was generated on an insulating substrate photolithographically from laser speckle pattern and the percolation conductance in two-dimensional conductor–insulator networks have been measured [23]. The observed anisotropy of the dc-conductance as a function of area fraction for metal was explained on the basis of the former model. In the latter anisotropic percolation model, on the contrary, it is shown that it has the same universality class as the isotropic percolation [13, 24] and the anisotropy of the macroscopic conductance is kept to be constant near the percolation threshold. On the other hand, Shklovskii pointed out that the topological anisotropy of the shape of dielectric regions in a metal with isotropic conductivity has anisotropic conductance near the percolation threshold [22]. Concerning to the anisotropy of the ac conductance of the anisotropic composite materials, however, it has not been studied yet as the authors know.

In our previous article [25], we studied the frequency characteristics of ac conductivity and dielectric constant of an isotropic two-dimensional random *RC*-network. The calculated frequency dependence succeeded in explaining the observed results [5, 6]. The purpose of this article is to clarify the frequency characteristics of the complex admittance tensor of an "anisotropic" two-dimensional random *RC*-network and to reveal the interrelation between the geometrical anisotropy and the anisotropy of the ac admittance. We calculate each component of the ac complex admittance tensor by applying a transfer matrix method [13]. We derive some exact analytical relations for each component of the complex admittance tensor. Finally, we clarify the range of applicability and limitation of the effective medium theory.

Model and analytical results

We adopt an anisotropic percolation model, which is an anisotropic two-dimensional square network consisting of two kinds of randomly placed conductors with scalar conductance, g_1 and g_2. The element $g_1 = 1/R$ is purely resistive and occurs with probabilities p_v and p_h in the vertical and the horizontal directions of the network, respectively. The second element is purely capacitive, $g_2 = j\omega C$, and occurs with probabilities $(1 - p_\mathrm{v})$ and $(1 - p_\mathrm{h})$ in the vertical and the horizontal directions. Here, j is an imaginary unit and ω is the angular frequency. The problem is to compute the complex admittance tensor per square of a large *RC*-network as a function of angular frequency ω. If R^{-1} is chosen as a unit of the admittance, $g_1 = 1$ with probabilities p_v and p_h, and $g_2 = jRC\omega$ with probabilities $(1 - p_\mathrm{v})$ and $(1 - p_\mathrm{h})$, in the vertical and the horizontal directions, respectively. Hence, the complex admittance tensor Y per square of a very large homogeneous network should be characterized by only three dimensionless parameters, p_v, p_h, and $RC\omega$, i.e., the complex admittance tensor per square can be expressed as $Y(p_\mathrm{v}, p_\mathrm{h}, RC\omega)$ in a unit of $1/R$. It should be mentioned that the horizontal diagonal component $Y_\mathrm{h}(p_\mathrm{v}, p_\mathrm{h}, RC\omega)$ can be calculated from the vertical diagonal component $Y_\mathrm{v}(p_\mathrm{v}, p_\mathrm{h}, RC\omega)$ as, $Y_\mathrm{h}(p_\mathrm{v}, p_\mathrm{h}, RC\omega) = Y_\mathrm{v}(p_\mathrm{h}, p_\mathrm{v}, RC\omega)$. Thus, the anisotropy of the complex admittance, $Y_\mathrm{v}(p_\mathrm{v}, p_\mathrm{h}, RC\omega)/Y_\mathrm{h}(p_\mathrm{v}, p_\mathrm{h}, RC\omega)$, can be calculated from the two vertical components, $Y_\mathrm{v}(p_\mathrm{v}, p_\mathrm{h}, RC\omega)$ and $Y_\mathrm{v}(p_\mathrm{h}, p_\mathrm{v}, RC\omega)$. From the real and the imaginary part of the vertical complex admittance, the vertical component of the effective conductance $\sigma_\mathrm{v}^{\mathrm{eff}}$ per square and the vertical component of the effective capacitance $C_\mathrm{v}^{\mathrm{eff}}$ per square (dielectric constant) can be obtained.

$$Y_\mathrm{v}(p_\mathrm{v},p_\mathrm{h},RC\omega) = \sigma_\mathrm{v}^{\mathrm{eff}}(p_\mathrm{v},p_\mathrm{h},RC\omega) + j\omega C_\mathrm{v}^{\mathrm{eff}}(p_\mathrm{v},p_\mathrm{h},RC\omega) \tag{1}$$

The following crossed relation is satisfied between $Y_\mathrm{v}(p_\mathrm{v}, p_\mathrm{h}, RC\omega)$ and $Y_\mathrm{v}(1 - p_\mathrm{v}, 1 - p_\mathrm{h}, (RC\omega)^{-1})$ in

geometrically equivalent condition for R and C regions in an any-dimensional RC-network [25].

$$Y_{\mathrm{v}}^{*}\left(1-p_{\mathrm{v}},1-p_{\mathrm{h}},\frac{1}{RC\omega}\right)=-\frac{j}{RC\omega}Y_{\mathrm{v}}(p_{\mathrm{v}},p_{\mathrm{h}},RC\omega) \quad (2)$$

From the above crossed relation, the next relation can be derived between the effective conductance and the effective capacitance.

$$\sigma_{\mathrm{v}}^{\mathrm{eff}}\left(1-p_{\mathrm{v}},1-p_{\mathrm{h}},\frac{1}{RC\omega}\right)R=C_{\mathrm{v}}^{\mathrm{eff}}(p_{\mathrm{v}},p_{\mathrm{h}},RC\omega)/C \quad (3)$$

On the other hand, for a two-dimensional isotropic homogeneous two-phase system, it is well known that the dual relation, $Y(c)Y(1-c)=g_1g_2$, holds between the scalar macroscopic complex admittances Y for complementary concentrations c and $(1-c)$, in geometrically equivalent condition [26]. Here, c is the concentration of the phase 1 of the two-phase system and g_1 and g_2 are the scalar conductance of the phases 1 and 2, respectively. We found that the dual relation can be extended for the complex admittance tensor of the anisotropic composite materials in geometrically equivalent condition. Indeed, it can be proved that the dual relation holds in the topologically anisotropic case for each diagonal component of the 2×2 macroscopic complex admittance tensor.

$$\begin{aligned}Y_{\mathrm{v}}(c)Y_{\mathrm{v}}(1-c)&=g_1g_2,\\ Y_{\mathrm{h}}(c)Y_{\mathrm{h}}(1-c)&=g_1g_2.\end{aligned} \quad (4)$$

The proof can be performed by following the similar procedure to that for the isotropic system [26], with a macroscopic 2×2 diagonal admittance tensor instead of a scalar macroscopic admittance. For the admittance per square of the anisotropic two-dimensional RC-network, the geometrically equivalent condition is satisfied and the dual relation holds for each component.

$$\begin{aligned}Y_{\mathrm{v}}(p_{\mathrm{v}},p_{\mathrm{h}},RC\omega)Y_{\mathrm{v}}(1-p_{\mathrm{v}},1-p_{\mathrm{h}},RC\omega)&=jRC\omega,\\ Y_{\mathrm{h}}(p_{\mathrm{v}},p_{\mathrm{h}},RC\omega)Y_{\mathrm{h}}(1-p_{\mathrm{v}},1-p_{\mathrm{h}},RC\omega)&=jRC\omega\end{aligned} \quad (5)$$

It should be mentioned that the dual relation does not hold for an anisotropic resistor model.

From Eqs. 2 and 5, the following reciprocal relations between the vertical components of the complex admittance tensor can be derived as well as the isotropic case [25].

$$Y_{\mathrm{v}}(p_{\mathrm{v}},p_{\mathrm{h}},RC\omega)Y_{\mathrm{v}}^{*}\left(p_{\mathrm{v}},p_{\mathrm{h}},\frac{1}{RC\omega}\right)=1 \quad (6)$$

The vertical complex admittance can be written as $Y_{\mathrm{v}}=|Y_{\mathrm{v}}|\exp(j\Phi_{\mathrm{v}})$. From the reciprocal relation Eq. 6, the following relations between the vertical complex admittances are obtained as well as the isotropic case [25].

$$\begin{aligned}|Y_{\mathrm{v}}(p_{\mathrm{v}},p_{\mathrm{h}},RC\omega)|&=\left|Y_{\mathrm{v}}\left(p_{\mathrm{v}},p_{\mathrm{h}},\frac{1}{RC\omega}\right)\right|^{-1}\\ \phi_{\mathrm{v}}(p_{\mathrm{v}},p_{\mathrm{h}},RC\omega)&=\phi_{\mathrm{v}}\left(p_{\mathrm{v}},p_{\mathrm{h}},\frac{1}{RC\omega}\right)\\ |Y_{\mathrm{v}}(p_{\mathrm{v}},p_{\mathrm{h}},1)|&=1\end{aligned} \quad (7)$$

On the other hand, the following relations between the vertical components of the complex admittance tensors for complementary concentrations are derived from the dual relation Eq. 5, as well as the isotropic case [25].

$$\begin{aligned}|Y_{\mathrm{v}}(p_{\mathrm{v}},p_{\mathrm{h}},RC\omega)||Y_{\mathrm{v}}(1-p_{\mathrm{v}},1-p_{\mathrm{h}},RC\omega)|&=RC\omega\\ \phi_{\mathrm{v}}(p_{\mathrm{v}},p_{\mathrm{h}},RC\omega)+\phi_{\mathrm{v}}(1-p_{\mathrm{v}},1-p_{\mathrm{h}},RC\omega)&=\frac{\pi}{2}\end{aligned} \quad (8)$$

For the anisotropic two-dimensional RC-networks, it is also known that the percolation threshold of the average bond occupation probability $p=(p_{\mathrm{v}}+p_{\mathrm{h}})/2$ is $p_{\mathrm{cr}}=0.5$ [13].

In the meanwhile, the vertical component Y_{v} of the complex admittance tensor per square of an anisotropic two-dimensional RC-network at p_{v}, p_{h}, and $RC\omega$ can be calculated approximately in the effective medium theory [27] as a solution of the following set of equations.

$$\begin{aligned}Y_{\mathrm{v}}&=\frac{p_{\mathrm{v}}(j\omega RC+S_{\mathrm{v}})+(1-p_{\mathrm{v}})j\omega RC(1+S_{\mathrm{v}})}{p_{\mathrm{v}}(j\omega RC+S_{\mathrm{v}})+(1-p_{\mathrm{v}})(1+S_{\mathrm{v}})},\\ S_{\mathrm{v}}&=R_{\mathrm{v}}^{-1}-Y_{\mathrm{v}}\\ R_{\mathrm{v}}&=\frac{1}{\pi^2}\int_0^{\pi}dk_1\int_0^{\pi}dk_2(1-\cos k_1)\\ &\quad[Y_{\mathrm{v}}(1-\cos k_1)+Y_{\mathrm{h}}(1-\cos k_2)]^{-1}.\end{aligned} \quad (9)$$

The similar set of equations can be written for the horizontal component Y_{h}. Equation 9 gives not only the exact percolation threshold of $p_{\mathrm{cr}}=0.5$, but also satisfies both the crossed relation of Eq. 2 and the dual relation of Eq. 5.

Numerical results

In the numerical calculation, we explore only the vertical component of the complex ac admittance tensor in a wide range of parameters, p_{v}, p_{h}, and $RC\omega$, since the horizontal component can be obtained by exchanging p_{v} and p_{h}. We use the exact analytical relations, Eqs. 7, 8, in order to check the calculation accuracy.

We compute the vertical component Y_{v} of the complex admittance per square of the anisotropic RC-network, using a transfer matrix method [13]. In the numerical studies, the network has a finite number of sites. Sizes of the square networks are set 200×200 and 500×500 at $p\neq 0.5$ and $p=0.5$, respectively, and the ensemble average was taken over 100 samples. All the calculated data present the average value with the standard deviation. We set the unit of the effective conductance $\sigma_{\mathrm{v}}^{\mathrm{eff}}$ as $1/R$ and that of the

effective capacitance as C. We set also the unit of the angular frequency ω as $1/RC$.

First, we show the dc effective conductance σ_v^{eff} as a function of resistors existence (bond occupation) probabilities, p_v and p_h. Two domains, insulating and metallic, of resistors existence probability, $p = (p_v + p_h)/2$, are apparent in Fig. 1a with the percolation threshold of $p_{cr} = 0.5$. The vertical dc effective conductance is very sensitive also to the anisotropy of the bond occupation probability and it becomes larger as the ratio of p_v to p_h increases at a fixed value of p. In the vicinity of the percolation threshold, however, the vertical dc conductance follows the power law, $\sigma_v^{eff} \propto (p - 0.5)^t$, with the same critical exponent of $t = 1.28$ [13, 24] irrespective of the anisotropy of the bond occupation probability, as seen in Fig. 1b. The anisotropy of dc conductance remains in the vicinity of the percolation threshold just as the topologically anisotropic system [22]. In Fig. 1a, the numerical results of the effective medium theory are also plotted by lines. It is seen that the effective medium theory always overestimates the dc effective conductance and the difference from the transfer matrix result becomes larger in the vicinity of the percolation threshold. As for the critical exponent, the effective medium theory gives $t = 1.0$ and cannot reproduce the correct critical exponent of $t = 1.28$.

Second, we will discuss the anisotropy of the dc conductance. In Fig. 2, we plot the ratio γ of the vertical component to the horizontal one, $\gamma = \sigma_v^{eff}(p_v, p_h, 0)/\sigma_h^{eff}(p_v, p_h, 0)$ as a function of p_v/p_h. The conductance ratio γ takes unity in the isotropic case and is suppressed less than p_v/p_h in the anisotropic case of $p_v/p_h < 1$. This means that the anisotropy of the effective conductance is much more enhanced than the geometrical anisotropy of the bond occupation probability. In Fig. 3, we plot the vertical component of the conductance in the extreme case of $p_h = 1$, $\sigma_v^{eff}(p_v, 1, 0)$, as a function of p_v. The effective conductance exhibits the power-law behavior with an exponent of 2.13 near the percolation threshold at $p_v = 0$. This is caused by the tortuous microscopic current path in the percolation. As for the horizontal component, on the other hand, $\sigma_h^{eff}(p_v, 1, 0) = 1$, since the microscopic current path is straight parallel to the horizontal direction. Hence, the conductance ratio γ in this extreme case is equal to $\gamma = \sigma_v^{eff}(p_v, 1, 0)$, and it is also much less than p_v for

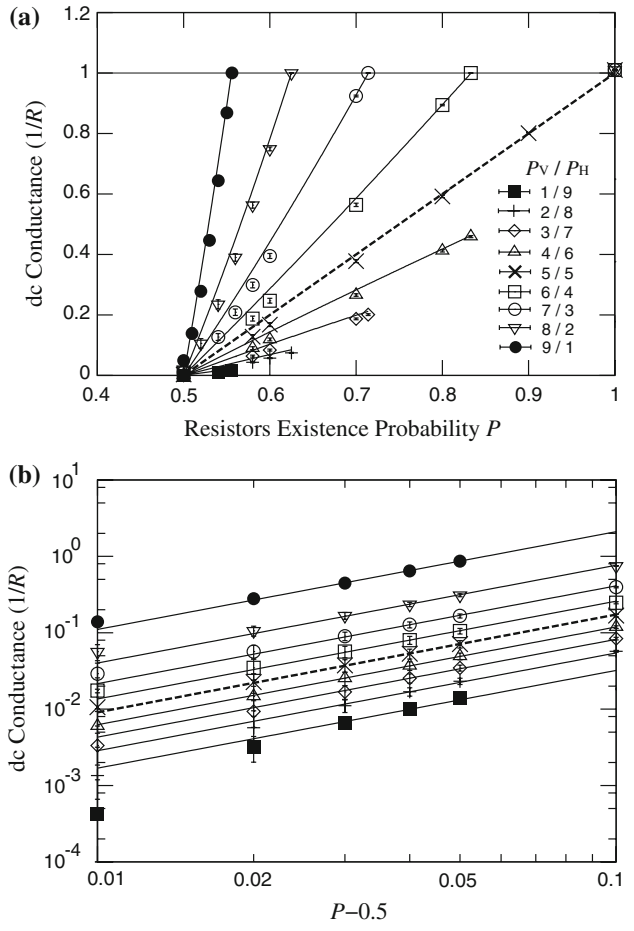

Fig. 1 The vertical dc conductance versus resistors existence probability p for several values of p_v/p_h. **a** The plot in a linear scale with the result of the effective medium theory (a *solid line* for the anisotropic case and a *broken line* for the isotropic case), and **b** the plot in a logarithmic scale with the predicted power law $\sigma_{eff} \propto (p - 0.5)^{1.28}$ (a *solid line* for the anisotropic case and a *broken line* for the isotropic case). The end of each line in (**a**) corresponds to $p_v = 1$ or $p_h = 1$

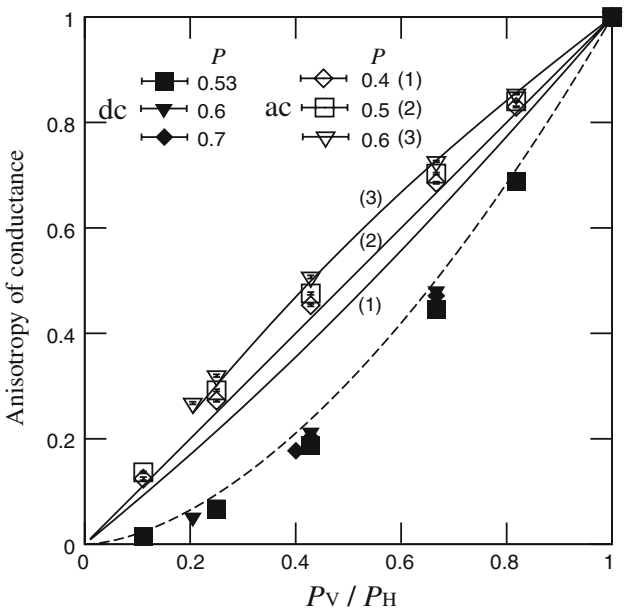

Fig. 2 Anisotropy of the effective conductance, $\sigma_v^{eff}(p_v, p_h, \omega RC)/\sigma_h^{eff}(p_v, p_h, \omega RC)$, versus p_v/p_h, for the dc effective conductance at $p = 0.53$, 0.6, and 0.7, and for the ac effective conductance at $\omega RC = 1$ for $p = 0.4$, 0.5, and 0.6. The relation of Eq. 10 for the anisotropy of the ac conductance at $\omega RC = 1$ and the relation of Eq. 11 for that of the dc conductance are plotted by *solid lines* and a *broken line*, respectively

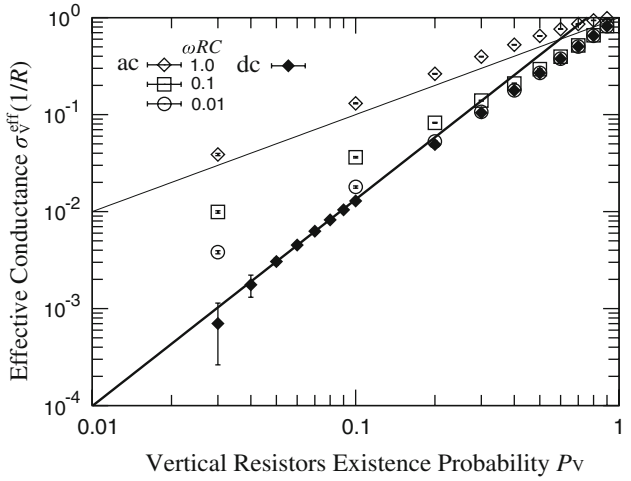

Fig. 3 The vertical effective conductance, $\sigma_v^{eff}(p_v, 1, \omega RC)$, versus p_v at $\omega RC = 0, 0.01, 0.1$, and 1, in the case of $p_h = 1$. Two relations, $\sigma_v^{eff} = p_v$ and $\sigma_v^{eff} = 1.8p_v^{2.13}$, are drawn by a *thin* and a *thick solid line*, respectively

$p_v \ll 1$. Figure 4 shows the map of the current intensity distribution [28] of both the vertical current and the lateral current at $p = 0.53$ for the case of $p_v = 0.212$ and $p_h = 0.848$. The vertical current path in Fig. 4a is very tortuous, but the lateral current path in Fig. 4b is rather straight. This difference between tortuosities of current paths is the origin of enhanced anisotropy of the effective conductance.

Next, we go on to the vertical component of the ac complex admittance tensor, $Y_v = |Y_v| \exp(j\Phi_v)$. Figure 5a–c shows the frequency characteristics of the magnitude $|Y_v|$ at $p = 0.4$, 0.5, and 0.6, for several ratios of the bond occupation probability. It should be mentioned that the vertical component takes values of $Y_v(1, p_h, RC\omega) = 1$ and $Y_v(0, p_h, RC\omega) = j\omega\ RC$, irrespective of values of p_h. Hence, the magnitude of the vertical component takes a constant value of 1 at $p_v = 1$ and does ωRC at $p_v = 0$. All the values of $|Y_v|$ for intermediate cases of $0 < p_v < 1$ are bounded between these two limiting lines. In the frequency range of $\omega RC < 1$, the magnitude of the vertical component increases as the ratio of p_v to p_h increases. We also observe that $|Y_v|$ has a value of unity at $\omega RC = 1$ irrespective of both p and the anisotropy p_v/p_h, as predicted by Eq. 7. Both the reciprocal and the dual relations of Eqs. 7, 8 are also satisfied in Fig. 5a–c. The corresponding frequency characteristics of the argument Φ_v are shown at $p = 0.4$, 0.5, and 0.6 in Fig. 5d–f, respectively. Figure 5d–f satisfy both the reciprocal and the dual relations of Eqs. 7, 8. In the metallic region of $p = 0.6$, the complex admittance takes the same phase with the voltage applied in both high and low frequencies. Thus, inphase current flows in the circuit and the circuit shows resistance characteristics. On the other hand, in the insulating region of $p = 0.4$, the

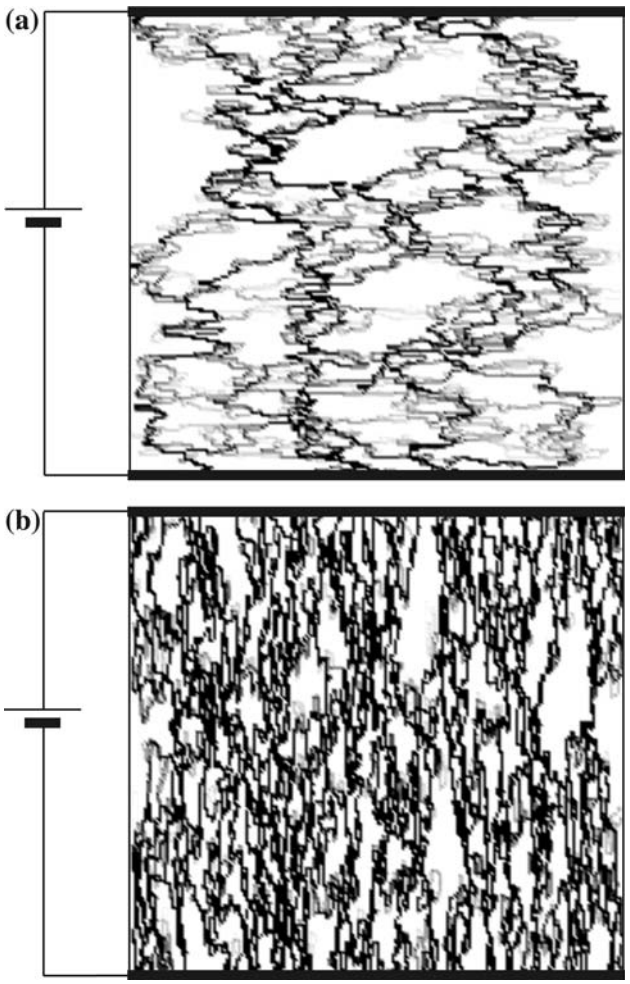

Fig. 4 Current intensity distribution in the linear gray scale at $p = 0.53$ for **a** $p_v = 0.212$ and $p_h = 0.848$ and **b** $p_v = 0.848$ and $p_h = 0.212$. Here, the current greater than the threshold was drawn by the most *black line* to clarify the current path

phase of the complex admittance shifts to $\pi/2$ from the voltage phase in both high and low frequencies; thus, the current that flows into the circuit is a $\pi/2$ shifted current. The circuit, then, shows capacitance characteristics. In the isotropic case, the argument is $\pi/4$ at the percolation threshold, and is always less than $\pi/4$ in the metallic region and greater than $\pi/4$ in the insulating region, taking the maximum or minimum at the frequency of $\omega RC = 1$ [25]. Mixing between resistance characteristics and capacitance characteristics maximizes at the frequency of $\omega\ RC = 1$, i.e., inverse of the relaxation time, in the isotropic case. The admittance argument is very sensitive to the anisotropy p_v/p_h in the frequency range of $0.01 < \omega RC < 100$, as shown in Fig. 5. In the anisotropic case, the argument in the metallic region can exceed $\pi/4$ for $p_v < p_h$ and that in the insulating region be reduced less than $\pi/4$ for $p_v > p_h$. At the percolation threshold, the argument becomes larger than $\pi/4$ for $p_v < p_h$ and smaller than $\pi/4$ for $p_v > p_h$.

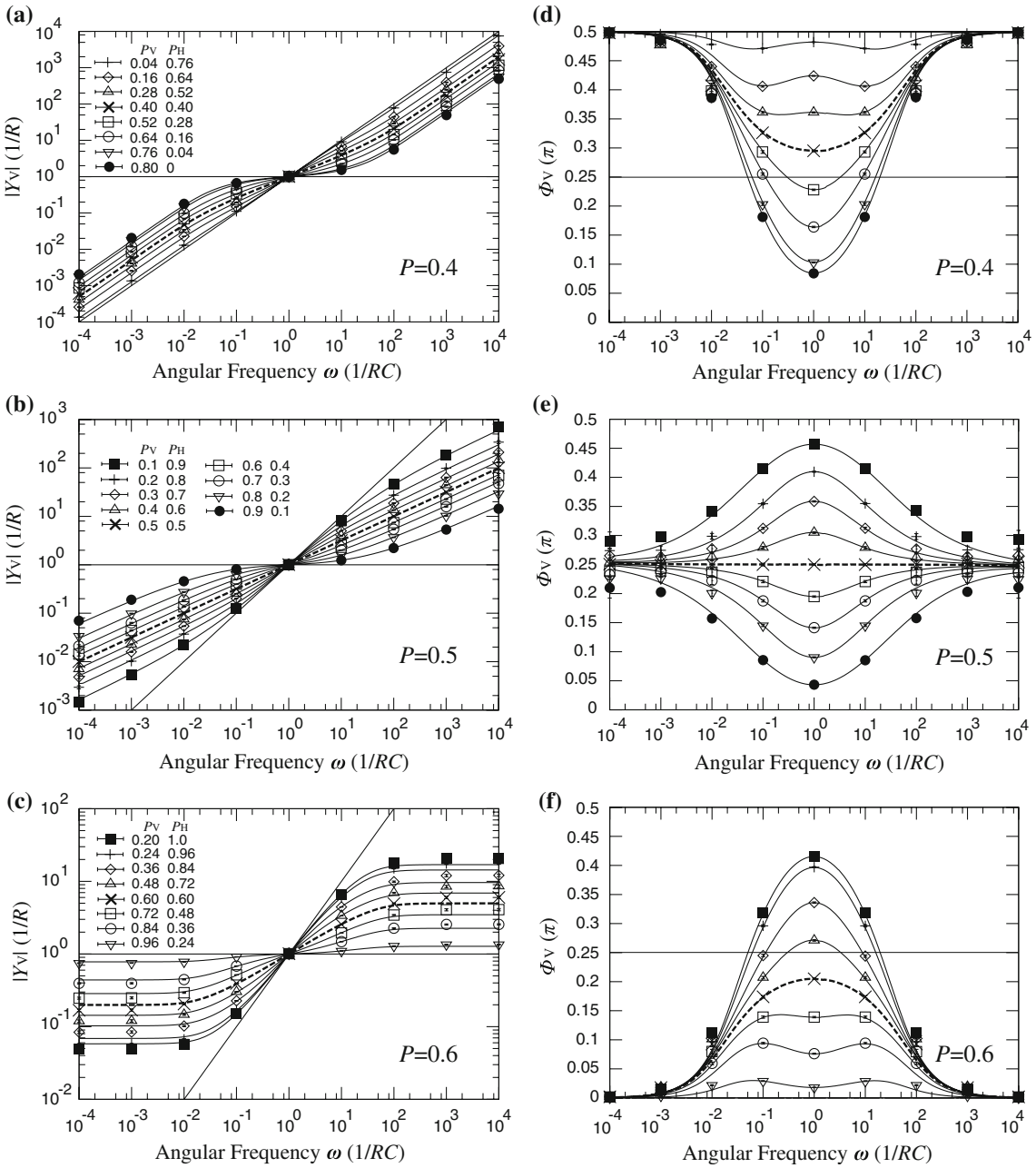

Fig. 5 Frequency characteristics of the magnitude $|Y_v(p_v, p_h, \omega RC)|$ at $p = 0.4$ (**a**), $p = 0.5$ (**b**), and $p = 0.6$ (**c**), and the argument $\Phi_v(p_v, p_h, \omega RC)$ at $p = 0.4$ (**d**), $p = 0.5$, (**e**) and $p = 0.6$ (**f**). The adopted values of p_v and p_h are written in **a**–**c**. The results of the effective medium theory are also plotted by a *solid line* for the anisotropic case and a broken line for the isotropic case

Figure 6a–c shows the frequency characteristics of the vertical component of the ac effective conductance at $p = 0.4$, 0.5, and 0.6, for several ratios of the bond occupation probability. When p is 0.5 at the percolation threshold in Fig. 6b, the effective conductance is given by $\omega^{0.5}$ in the isotropic case [25]. As the ratio p_v/p_h increases, the effective conductance is increased in the frequency region of $\omega RC < 1$ and the frequency dependence can be described as $\alpha\omega^{0.5}$ in the low frequency region. α increases with increasing p_v/p_h as seen in Fig. 6b. As for the insulating case of $p = 0.4$, the effective conductance approaches to 0 in proportion to ω^2 for $\omega RC \ll 1$ because of the dual relation of Eq. 5. In the opposite metallic condition of $p = 0.6$, the effective conductance comes to a constant finite value in low frequencies. As the ratio p_v/p_h increases, the effective conductance increase monotonically in the frequency range of $\omega RC < 1$, since meander of the microscopic current path is suppressed. On the other hand, the frequency characteristics of the effective capacitance (dielectric constant) are shown in Fig. 6d–f. The

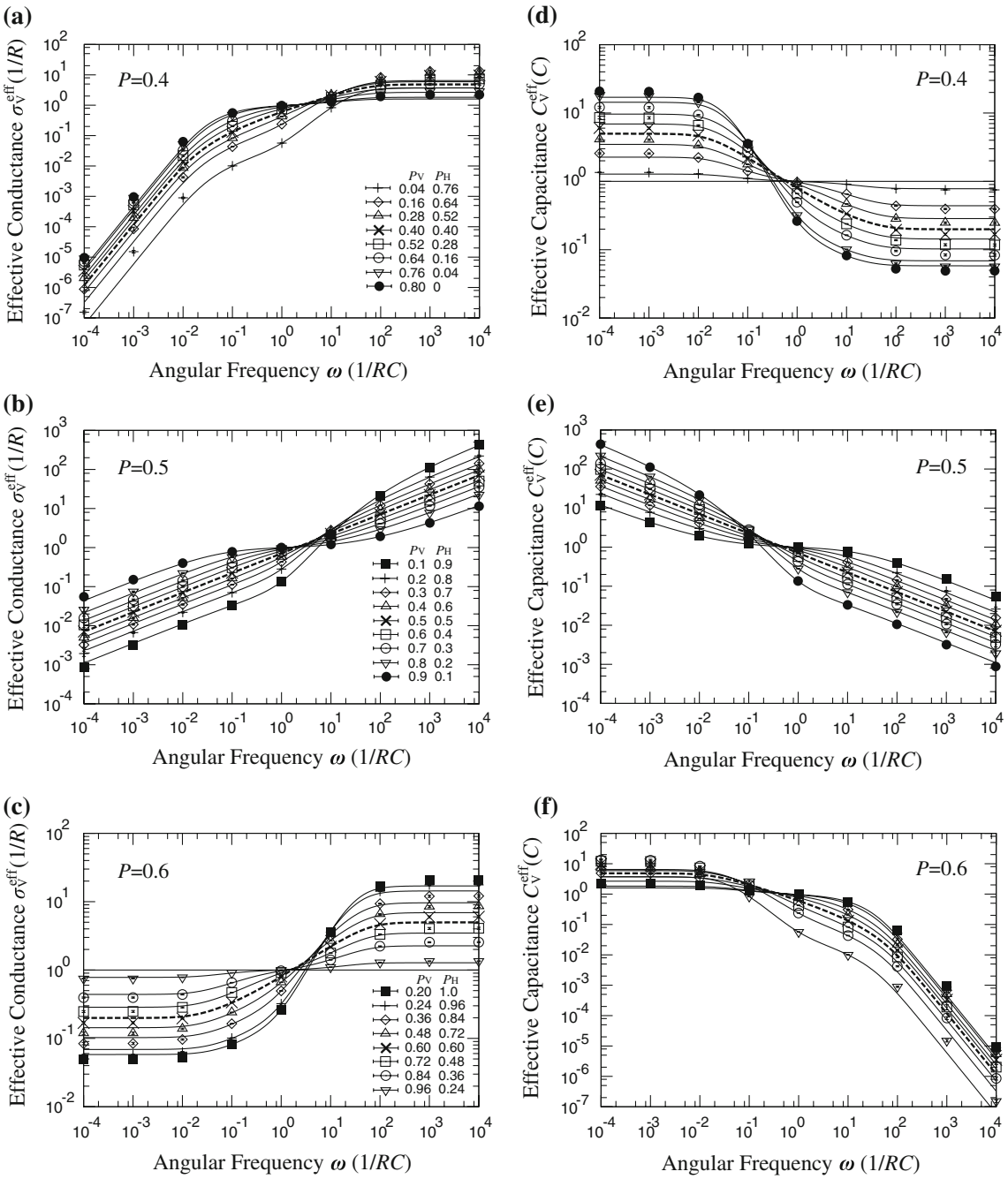

Fig. 6 Frequency characteristics of the vertical component $\sigma_v^{eff}(p_v, p_h, \omega RC)$ of the ac effective conductance tensor at $p = 0.4$ (**a**), $p = 0.5$ (**b**), and $p = 0.6$ (**c**), and the vertical component $C_v^{eff}(p_v, p_h, \omega RC)$ of the ac effective capacitance tensor at $p = 0.4$ (**d**), $p = 0.5$ (**e**), and $p = 0.6$ (**f**). The adopted values of p_v and p_h are written in (**a**), (**b**), and (**c**). The results of the effective medium theory are plotted by a *solid line* for the anisotropic case and by a *broken line* for the isotropic case

effective capacitance is related to the effective conductance through the relation of Eq. 3.

As for the conductance anisotropy γ of the ac conductance, the ratio of the vertical component at $\omega RC = 1$ to the horizontal one, $\gamma = \sigma_v^{eff}(p_v, p_h, 1)/\sigma_h^{eff}(p_v, p_h, 1)$, is plotted at $p = 0.4$, 0.5, and 0.6 in Fig. 2. The ratio γ is approximately equal to $\gamma \simeq p_v/p_h$, in contrast with the dc conductance. In Fig. 3, we plot the vertical component of the effective conductance in the extreme case of $p_h = 1$, $\sigma_v^{eff}(p_v, 1, \omega RC)$, at $\omega RC = 1$, 0.1, and 0.01. $\sigma_v^{eff}(p_v, 1, 1)$ is nearly equal to p_v and $\sigma_v^{eff}(p_v, 1, \omega RC)$ decreases with decreasing ωRC from 1. This implies that the microscopic

current path changes with frequency from the approximately straight path in the vertical direction at $\omega RC = 1$ toward the tortuous path at the dc limit.

Discussion and conclusion

First, we will discuss the anisotropy of the ac conductance at $\omega RC = 1$ in Fig. 2. The conductance of resistors and that of capacitors have the same magnitude of unity at $\omega RC = 1$, and the microscopic current flows mainly parallel to the macroscopic current direction. Hence, the argument Φ_v at $\omega RC = 1$ is approximated as, $\Phi_v \simeq \arctan(p_v^{-1} - 1)$, irrespective of values of p_h. In Fig. 7, this relation is plotted as a function of p_v with calculated values of Φ_v at $\omega RC = 1$ in Fig. 5. It is seen that their agreement is fairy good. On the other hand, $|Y_v| = 1$ at $\omega RC = 1$ and the vertical effective conductance is approximated as, $\sigma_v^{\text{eff}}(p_v, p_h, 1) \simeq p_v/\sqrt{p_v^2 + (1-p_v)^2}$. Thus, the anisotropy can be approximated by the relation

$$\frac{\sigma_v^{\text{eff}}(p_v, p_h, 1)}{\sigma_h^{\text{eff}}(p_v, p_h, 1)} = \frac{p_v\sqrt{p_h^2 + (1-p_h)^2}}{p_h\sqrt{p_v^2 + (1-p_v)^2}}. \quad (10)$$

The predicted anisotropy of the effective conductance at $\omega RC = 1$ is plotted by a solid line in Fig. 2. It is seen that Eq. 10 can explain fairly well the calculated behavior by a transfer matrix method in a metallic region, although there exists some discrepancy in the insulating region.

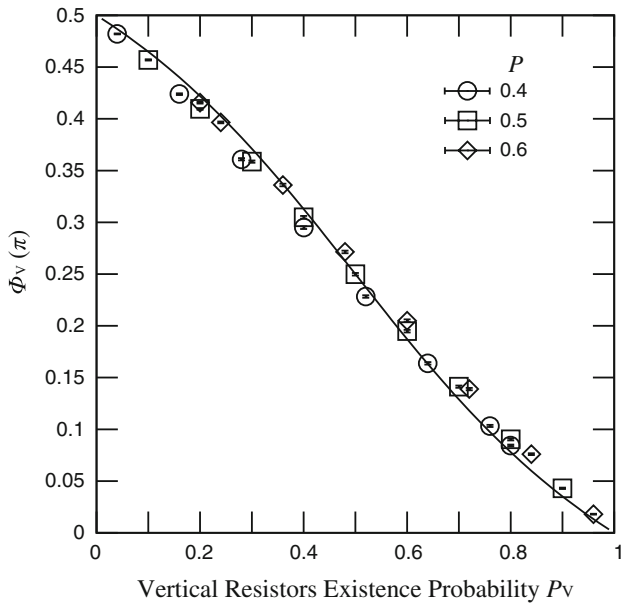

Fig. 7 The argument $\Phi_v(p_v, p_h, \omega RC)$ of the vertical component of the complex admittance tensor at $\omega RC = 1$ as a function of p_v, for three values of p. The relation, $\Phi_v = \arctan(p_v^{-1} - 1)$, is plotted by a *solid line*

Second, we will discuss the anisotropy of the dc conductance in Fig. 2. The vertical component of the dc conductance can be given by the power law in the vicinity of the percolation threshold in Fig. 1b as, $\sigma_v^{\text{eff}}(p_v, p_h, 0) \simeq \beta(p_v/p_h)(p - 0.5)^{1.28}$. Here, the coefficient β is assumed to be a function of the bond occupation anisotropy. On the other hand, the relation, $\sigma_v^{\text{eff}}(p_v, 1, 0) \simeq 1.8 p_v^{2.13}$, holds in the vicinity of the percolation threshold in Fig. 3. Hence, the function β can be determined as $\beta(p_v) = 1.8 \times 2^{1.28} \times p_v^{0.85}$ for $p_v \ll 1$. Therefore, the anisotropy of the dc conductance can be written in the vicinity of the percolation threshold as

$$\frac{\sigma_v^{\text{eff}}(p_v, p_h, 0)}{\sigma_h^{\text{eff}}(p_v, p_h, 0)} = \left(\frac{p_v}{p_h}\right)^{1.70}. \quad (11)$$

The predicted anisotropy of the dc conductance is plotted by a broken line in Fig. 2. The relation of Eq. 11 can explain the calculated behavior in the vicinity of the percolation threshold.

Finally, we compare our numerical results on the vertical component of the ac admittance with the effective medium theory. The vertical component of the ac admittance in the effective medium theory are also plotted in Figs. 5, 6. The effective medium theory can reproduce well the calculated results by the transfer matrix method in the frequency range of $10^{-1} \leq \omega RC \leq 10$. This means that the effective medium theory works well when the conductance of two components have a similar magnitude. However, the effective medium theory cannot reproduce the percolative nature. In the frequency range of $\omega RC \leq 0.01$, the effective medium theory always overestimates the effective conductance in the metallic region and underestimates the effective capacitance in the insulating region, as seen in Fig. 6c, d. The discrepancy increases as p_v decreases in the metallic region, while it increases as p_v increases in the insulating region. The discrepancy is caused by increase of meander in the microscopic current path. The degree of meandering of the microscopic current path through resistors increases as p_v decreases in the metallic region, while one through capacitors increases as p_v increases for the vertical macroscopic current in the insulating region. Hence, the discrepancy with the effective medium theory is enlarged as the anisotropy of the bond occupation probabilities increases. To see more quantitatively, we plot the effective capacitance for the insulating region in the linear scale in Fig. 8. The effective medium theory always underestimate the effective capacitance in a frequency range of $\omega RC \leq 0.01$ in the insulating region, compared to the numerical result by a transfer matrix method. The discrepancy increases as the average bond occupation

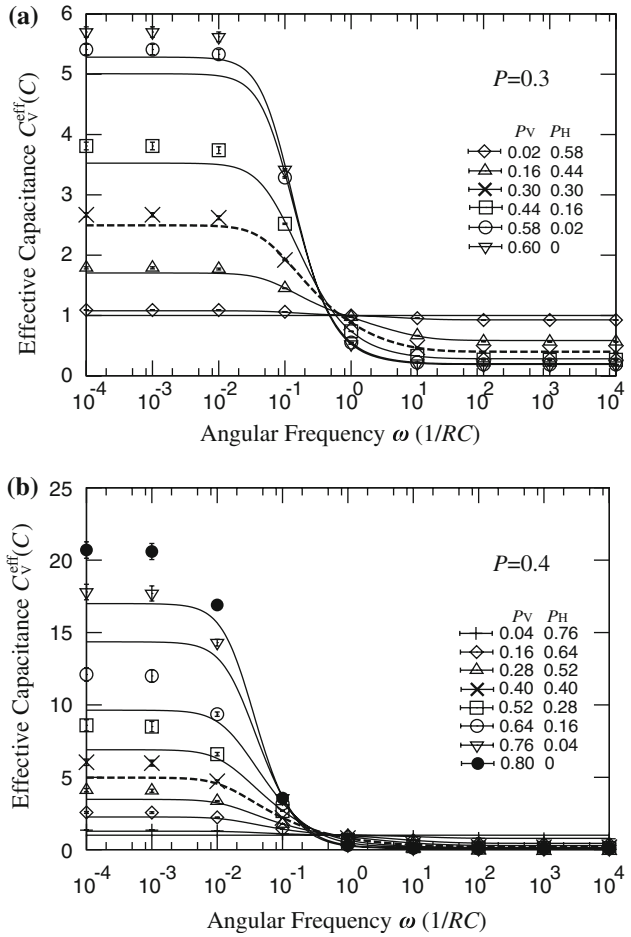

Fig. 8 Frequency characteristics of the vertical ac effective capacitance at $p = 0.3$ (**a**) and $p = 0.4$ (**b**) in the linear scale. The adopted values of p_v and p_h are written in (**a**) and (**b**). The results of the effective medium theory are plotted by a *solid line* for the anisotropic case and a broken line for the isotropic case

probability p approaches the percolation threshold or as p_v is increased, as seen in Fig. 8.

In summary, we study the ac complex admittance tensor (ac conductivity and dielectric constant) of an anisotropic two-dimensional *RC*-network using a transfer matrix method and reveal the dependence on the anisotropy of the bond occupation probabilities. It is found that the dual relation holds in each component of the complex admittance tensor of the anisotropic two-dimensional *RC*-network, as well as the scalar admittance in the isotropic *RC*-network. For both the effective ac conductance in the metallic region and the effective ac capacitance in the insulating region, the anisotropy is most enhanced at the dc limit and suppressed around $\omega RC = 1$. The anisotropy of the dc conductance is given by a power law of the ratio of the bond occupation probabilities in two directions in the vicinity of the percolation threshold and is much more enhanced than the anisotropy of the bond occupation probabilities. The enhanced anisotropy at the dc limit is caused by meander of the microscopic current path. The anisotropy of the ac conductance at $\omega RC = 1$ is nearly equal to the anisotropy of the bond occupation probability, owing to nearly straight microscopic current path parallel to the macroscopic current direction. The effective medium theory always overestimates the effective conductance in the metallic region and underestimates the effective capacitance in the insulating region in the frequency range of $\omega RC \leq 10^{-2}$ and the discrepancy is increased with degree of meandering of the microscopic current path.

Acknowledgements We acknowledge Dr. Shigeru Kohinata in Sumitomo Metal Mining Co. for stimulating discussion on high frequency conductance on conductive epoxy adhesive.

References

1. Nakai T, Shimoji T, Tanaka M, Nakajima K, Kohinata S (1994) Proceedings of the eighth international microelectronics conference, p 167
2. Song Y, Noh TW, Lee S-I, Gaines JR (1986) Phys Rev B 33:904
3. Wu J, McLachlan DS (1998) Phys Rev B 58:14880
4. Chiteme C, McLachlan DS (2003) Phys Rev B 67:024206
5. Jhans H, Kim D, Rasmussen RJ, Honig JM (1996) Phys Rev B 54:11224
6. Chiteme C, McLachlan DS, Sauti G (2007) Phys Rev B 75: 094202
7. Bergman DJ (1992) Solid State Phys 46:147
8. Landauer R (1952) J Appl Phys 23:779
9. Kirkpatrick S (1973) Rev Mod Phys 45:574
10. Efros AL, Shklovskii BI (1976) Phys Stat Sol b 76:475
11. Bergman DJ, Imry Y (1977) Phys Rev Lett 39:1222
12. Bergman DJ, Imry Y (1981) Phys Rev Lett 14:855
13. Derrida B, Vannimenus J (1982) J Phys A 15:L557
14. Wilkinson D, Langer JS, Sen PN (1983) Phys Rev B 28:1081
15. Newman MEJ, Ziff RM (2000) Phys Rev Lett 85:4104
16. Yoshida K, Tomi Y, Ueda S (1988) Jpn J Appl Phys 27:2224
17. Dianoux R, Smilde HJH, Marchi F, Buffet N, Mur P, Comin F, Chevrier J (2005) Phys Rev B 71:125303
18. Stankovich S, Dikin DA, Dommett GHB, Kohlaas KM, Zimney EJ, Stach EA, Piner RD, Nguyen ST, Ruoff RS (2006) Nature 442:282
19. Grujicic M, Cao G, Roy WN (2004) J Mater Sci 39:4441. doi: 10.1023/B:JMSC.0000034136.11779.96
20. Du F, Fisher JE, Winey KI (2005) Phys Rev B 72:121404(R)
21. Lobb CJ, Frank DJ, Tinkham M (1981) Phys Rev B 23:2262
22. Shklovskii BI (1978) Phys Stat Sol b 85:K111
23. Smith LN, Lobb CJ (1979) Phys Rev B 20:3653
24. Nakanishi H, Reynols PJ, Render S (1981) J Phys A 14:855
25. Murtanto TB, Natori S, Nakamura J, Natori A (2006) Phys Rev B 74:115206
26. Dykhne AM (1971) Sov Phys JETP 32:63
27. Bernasconi J (1974) Phys Rev B 9:4575
28. Bergman DJ, Duering E, Murat M (1990) J Stat Phys 58:1